Wind and Structures, Vol. 15, No. 6 (2012) 481-494
DOI: http://dx.doi.org/10.12989/was.2012.15.6.481

Calculated external pressure coefficients on livestock buildings and comparison with Eurocode 1

D.L. Kateris[1], V.P. Fragos[1,2], T.A. Kotsopoulos*[1,2], A.G. Martzopoulou[3] and D. Moshou[1]

[1]*Department of Hydraulics, Soil Sciences and Agricultural Engineering, Aristotle University of Thessaloniki Thessaloniki, Greece*
[2]*Agricultural Structures Control Center (ASCC),Thermi-Thessaloniki, Greece*
[3]*School of Architecture, Aristotle University of Thessaloniki, Thessaloniki, Greece*

(Received February 1, 2012, Revised May 24, 2012, Accepted June 20, 2012)

Abstract. The greenhouse type metal structures are increasingly used in modern construction of livestock farms because they are less laborious to construct and they provide a more favorable microclimate for the growth of animals compared to conventional livestock structures. A key stress factor for metal structures is the wind. The external pressure coefficient (c_{pe}) is used for the calculation of the wind effect on the structures. A high pressure coefficient value leads to an increase of the construction weight and subsequently to an increase in the construction cost. The EC1 in conjunction with EN 13031-1:2001, which is specialized for greenhouses, gives values for this coefficient. This value must satisfy two requirements: the safety of the structure and a reduced construction cost. In this paper, the Navier – Stokes and continuity equations are solved numerically with the finite element method (Galerkin Method) in order to simulate the two dimensional, incompressible, viscous air flow over the vaulted roofs of single span and twin-span with eaves livestock greenhouses' structures, with a height of 4.5 meters and with length of span of 9.6 and 14 m. The simulation was carried out in a wind tunnel. The numerical results of pressure coefficients, as well as, the distribution of them are presented and compared with data from Eurocodes for wind actions (EC1, EN 13031-1:2001). The results of the numerical experiment were close to the values given by the Eurocodes mainly on the leeward area of the roof while on the windward area a further segmentation is suggested.

Keywords: Eurocode; external pressure coefficient; CFD; livestock building; wind flow

1. Introduction

Livestock buildings are mainly heavy structures made by either concrete blocks or reinforced concrete. Nowadays, due to the advantages of steel in building construction (easier formation of the frame, better ventilation and lighting etc), more and more constructions that are destined for animal housing have metal frame (Kotsopoulos and Martzopoulou 2007, Nikita-Martzopoulou 2007). These structures because of their greenhouse frame are mentioned as Livestock Greenhouse Buildings (LGBs).

With the recent rise in steel price and a probable further increase of it in the future (LME 2011) significant proportion of the total construction cost is the expense for the steel. One of the main

* Corresponding author, Lecturer, E-mail: mkotsop@agro.auth.gr

stress factors of the metal construction is the wind. For the calculation of the structures' load by the wind, the external wind pressure coefficient is used. The wind pressure coefficient is obtained from the EC1 (CEN 2005) in conjunction with the EN 13031-1:2001 (CEN 2001), which is specialized for greenhouses. The use of the Eurocodes is expected to become mandatory in 2011 by the EU Member States (European Commission website on the Eurocodes). In Greece the use of the Eurocodes is already obligatory by the ASCC*. A rise of the pressure coefficient value results in increased construction costs, because the amount of steel that has to be used for reinforcing the static integrity of the structure against the wind, will be higher. It has to be noted that many greenhouse-type livestock buildings' constructors complain about the implementation of Eurocodes leads to heavy structures (personal communication with manufacturers in Greece).

The safety of the structures is of major importance but the cost of the construction must not be overlooked, particularly as far as livestock buildings are concerned, as livestock farming is an agro-business sector that faces financial problems. Therefore, a reliable experimental and/or a computational approach for estimating the pressure coefficient is required, as well as, performing an analysis of its distribution on the roof of the structure. It has to be noted that the greenhouse structures belong to the general category of the low-rise buildings (Mistriotis and Briassoulis 2002).

The distribution of pressure coefficients for various geometrical low-rise buildings is obtained by full-scale or wind-tunnel numerical simulations and experiments (Robertson *et al.* 2002, Ginger and Holmes 2003, Tieleman 2003, Blackmore and Tsokri 2006, Guirguis *et al.* 2007, Lopes *et al.* 2010, Kozmar 2011). The full-scale experiments as well as experiments using air-tunnels are more reliable for the detection of the pressure distributions, however, their implementation cost is high and they are not applicable to every structure. Alternatively, the pressure distribution can be estimated using computational and numerical models. The numerical models have proven their value for the design of livestock buildings (Norton *et al.* 2009). Up to now many researchers have studied the c_p distributions computationally. Reichrath and Davies (2002) have used the commercial CFD package Fluent 5.3.18 in order to estimate the pressure distribution on a 7 span Venlo-type glasshouse. Wright and Easom (2003) have used a non-linear *k–e* model to find the pressure coefficient on a surface mounted cube. Shklyar and Arbel (2004) have used a standard *k–e* model and RSM model to predict the pressure coefficient distribution on a pitched-roof greenhouse.

Nevertheless, few works exist that compare pressure coefficients obtained either computationally or experimentally, with the Eurocodes on low-rise buildings (Blackmore and Tsokri 2006, Mistriotis and Briassoulis 2002, Robertson *et al.* 2002), although the use of Eurocodes will shortly be mandatory for EU Member States.

Furthermore, to the author's best knowledge up to now, there is no work outlining the c_{pe} over the vaulted roofs of single span and twin-span with eaves livestock greenhouses' structures with length of span 9.60 and 14 m although, usually, the span of greenhouse type livestock buildings ranges between the above numbers, for functional reasons.

In the light of the above developments, pressure coefficients are calculated with a Computational Fluid Dynamics (CFD) model developed and designed by the research team of ASCC. This model simulates air flow inside an air-tunnel with the appropriate boundary conditions. The two dimensional, incompressible, viscous air flow is simulated over the vaulted roofs of single span and

*Agricultural Structures Control Center (ASCC), in Thessaloniki is the official authority to provide certificate of quality of greenhouse – type livestock buildings to the constructors and importers of these structures, in Greece.

twin-span with eaves livestock greenhouses' structures with length of span 9.6 and 14 m and with a height of 4.5 m. The calculated wind pressure coefficients are compared and discussed with the corresponding values given by the Eurocodes. This paper looks through the discussion of the results and the comparison with the data of the Eurocodes for the pressure coefficients (c_p) to yield useful conclusions which will help to gain a better understanding of the pressure distribution on livestock buildings. In addition, streamlines and distributions of the speed components (contours of stream-wise velocity and cross-wise velocity) over the computational flow field are presented in order to provide a complete picture of the flow configuration which affects the pressure distribution. The results of this study will be useful for agricultural engineers in the design of livestock buildings.

2. Materials and methods

2.1 Geometries of structures that have been used for the computational model

Vaulted roofs greenhouse with eaves buildings are widely used for housing livestock and therefore such geometries were used in this computational study. According to the ASCC data, the length of span of these structures range from 9.6 m to 14 m and their height comes up to 4.5 m (Greek regulations). Typically, these structures are either single- or twin-span. The structures selected in this study meet the above dimensions having 4.5 m height and length of span 9.6 to 14 m and they are either single- or twin-span. Each case was defined as follows: ($LGB^1_{9.6}$) ($LGB^1_{14.0}$) ($LGB^2_{9.6}$) ($LGB^2_{14.0}$), where the subscript indicates the span while the superscript indicates the number of spans.

In the present work, the air flow was simulated in a wind tunnel over scaled models of these structures. The scaled models meet proportionally the dimensions of the livestock structures mentioned above. The proportions of the models are described in detail in section 2.2.2.

2.2 The CFD model

The numerical simulation of the studied flow was based on the solution of the Navier - Stokes and continuity equations and on the determination of the boundary conditions of the computational flow field (wind tunnel). The finite element code used to solve the equations was developed by using the programming language Fortran.

The particular mathematical model has been used and validated against experimental data in the study (Fragos *et al.* 1997) for flow simulation around a rectangular obstacle. Moreover, it has been used and verified in the study (Psychoudaki *et al.* 2005) for flow simulation around a parabolic obstacle and in the study (Dados *et al.* 2011) for flow simulation over two successive tunnel greenhouses.

Details of the mathematical model and its solution are described in the following sections.

2.2.1 Governing equations

The dimensionless Navier-Stokes (1) and continuity (2) equations are used to solve the two-dimensional, viscous, incompressible, steady flow over four different greenhouse's structures inside a wind tunnel

$$U\nabla U = -\nabla p + \frac{1}{Re}\nabla^2 U \quad (1)$$

$$\nabla U = 0 \quad (2)$$

Where, $U = (u,v)$ is the velocity vector of the fluid with u and v its components in the x and y direction respectively, p is the pressure and Re is the Reynolds number. The governing equations have been rendered dimensionless by using the following characteristic magnitudes (L,V, P_o, Re), where L is the length of the ridge above ground level (m), V is the uniform approaching velocity of the fluid (inlet free stream velocity, ms^{-1}), $P_o = \rho V^2$ is the pressure intensity (Nm^{-2}), ρ is the density of the fluid (Ns^2m^{-4}), $Re = VLv^{-1}$ is the Reynolds number and v is the kinematic viscosity of the fluid (m^2s^{-1}).

2.2.2 Computational domain - boundary conditions

The wind tunnel and structures dimensions for all cases are presented in Table 1. The boundary conditions, as well as, the computational domain used in this work are shown in Fig. 1.

A uniform free stream flow is used as boundary condition at the entrance of the computational domain (John and Liakos 2006). The no-slip boundary conditions are imposed along the walls of the wind tunnel and livestock greenhouse structure. At the outlet, free boundary condition has been applied in order to let the fluid to leave the computational domain freely, without any distortion (Malamataris 1991, Papanastasiou *et al.* 1992).

2.2.3. Numerical solution of the mathematical model

2.2.3.1 Finite element formulation – spatial advancements

The standard Galerkin finite element method was used in order to solve the governing Eqs. (1) and (2) along with the appropriate boundary conditions (Zienkiewicz *et al.* 2006).

The pressure is formulated by a linear basis function, while the velocity by a quadratic one. The

Table 1 Computational data of the scale structures and of the wind tunnel

	$LGB^1_{9.6}$	$LGB^1_{14.0}$	$LGB^2_{9.6}$	$LGB^2_{14.0}$
Number of vaulted roofs	1	1	2	2
L^a	1L	1L	1L	1L
h^b	0.555L	0.555L	0.555L	0.555L
f^c	0.444L	0.444L	0.444L	0.444L
d^d	2.133L	3.111L	2.133L	3.111L
hd^{-1}	0.260	0.179	0.260	0.179
fd^{-1}	0.208	0.143	0.208	0.143
Location of greenhouse	5L	5L	5L	5L
Length of wind tunnel	30L	30L	30L	30L
Height of wind tunnel	8L	8L	8L	8L

[a] length of the ridge above ground level.
[b] length of column (between foundation and gutter).
[c] length between gutter and ridge.
[d] length of span.

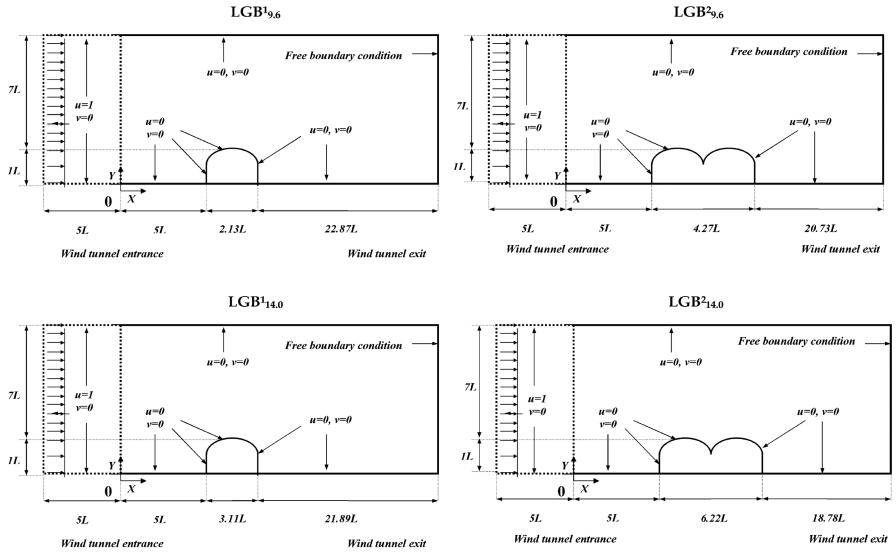

Fig. 1 Computational domain and boundary conditions of the two-dimensional flow over the livestock greenhouse structures.

unknown velocities and pressure are expanded in Galerkin basis functions. Eqs. (1) and (2) are weighted integrally with the basis functions. By applying the divergence theorem, the weighted residuals (R_c^i, R_M^i) become

$$R_c^1 = \int_V \nabla U \, \Psi^i dV \tag{3}$$

$$R_M^i = \int_V \left[\mathrm{U}\nabla U - \nabla\left(-pI + \frac{1}{Re}T\right)\right]\Phi^{\mathrm{i}}\mathrm{dV} - \int_S \left[-\mathrm{pI} + \frac{1}{Re}T\right]\Phi^i dS \tag{4}$$

Where, I is the identity matrix; $T = \nabla U + (\nabla U)^T$ is the stress tensor of the Newtonian fluid; Ψ^{i}, Φ^{i} are the linear and quadratic basis functions in Eqs. (3) and (4) respectively; V is the volume of the element and S is the surface of it. The non linear system of Eqs. (3) and (4) is solved numerically with the Newton-Raphson method. The essential (Dirichlet type) boundary conditions (u = 0 or 1 and v = 0) are applied to all boundaries of the domain, except for the outflow. The integral over the volume of the Eq. (4) is calculated to all nodes of the computational domain. At the nodes of the domain exit, the free boundary condition is applied and all the integrals of the Eq. (4) are calculated.

2.2.3.2 Computational meshes

The computational mesh consisted from triangular and rectangular elements. The density of meshes is checked because it is an important factor with respect to the accuracy of the solution and the computational effort and time. Further densification of the mesh resulted in no significant change in the solution. The computational meshes in the flow field are shown in Fig. 2, while the details of them are given in Table 2.

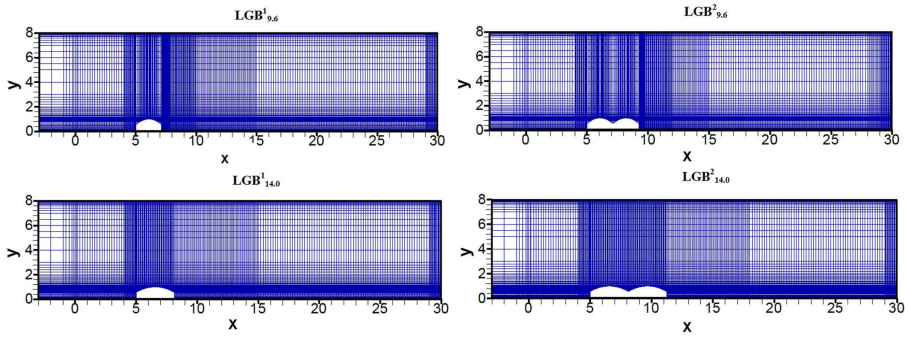

Fig. 2 Computational meshes used in this work.

Table 2 Data of the computational meshes and the CPU time per iteration

	$LGB^1_{9.6}$	$LGB^1_{14.0}$	$LGB^2_{9.6}$	$LGB^2_{14.0}$
Number of elements	27443	19320	27307	18312
Number of nodes	110577	77893	109077	73783
Number of unknowns	249023	175437	247682	166194
CPU time per iteration (min)	4.64	3.85	4.21	3.52

2.2.3.3 Finite element code

The finite element code that had been used by Fragos *et al.* (1997), was properly modified with respect to the configuration of the mesh in order to adjust it according to the geometries of the structures examined in this work. At each node of the finite elements, the unknown variables of the stream-wise (u) and the cross-wise (v) velocities are numerically calculated. Also, the pressure is calculated at the edge nodes of the finite elements. The convergence criterion imposed on the Newton–Raphson iteration was 10^6 for velocities and $5{\cdot}10^4$ for pressure. Gauss elimination is used for the inversion of the Jacobian matrix, which is formed by differentiating the residuals R_c^i and R_M^i with respect to the nodal unknowns u, v and p. The finite element code was executed for Reynolds numbers (Re) of 10, 30, 50, 80, 100, 500, 1000, 1370 and 1500. Data of the CPU time per iteration for all cases are presented in Table 2.

2.3 Pressure coefficient calculation

The determination of the external pressure coefficient on the roof of livestock buildings was based on the pressure values that were calculated by solving the equations of the mathematical model (1-4). The equation used to calculate the external pressure coefficient is the following

$$c_{pe} = 2(p - p_o) \tag{5}$$

Where, c_{pe} is the external pressure coefficient, p is the pressure on the roof of the building, calculated by the Finite element code and p_o is the reference value of pressure.

3. Results – discussion

3.1 Streamlines – components of velocity

The streamlines and the components of velocity (u and v) are presented in order to provide a complete picture of the configuration of the flow over the structures. They are presented for two indicative numbers Re (100 and 1000) throughout their computational flow field. The streamlines for the cases ($LGB^1_{9.6}$) ($LGB^1_{14.0}$) ($LGB^2_{9.6}$) ($LGB^2_{14.0}$) are illustrated in Fig. 3.

It has been noticed that the reattachment length, formed downstream, increases when the number of Reynolds increases too. The same conclusion was reached by other researchers that studied different obstacles geometries in steady flow conditions (Armaly *et al.* 1983, Boum *et al.* 1999, Hong *et al.* 1991). In the present work, it is found that for the same Re number, the reattachment length downstream the livestock buildings is reduced when the length of span of the structure increases. The above finding agrees with Antoniou and Bergeles (1988) who showed experimentally that by increasing the ratio of length to height the reattachment length is reduced.

Fig. 4 shows the distribution of the horizontal component of velocity for the cases ($LGB^1_{9.6}$) ($LGB^1_{14.0}$) ($LGB^2_{9.6}$) ($LGB^2_{14.0}$). It is obvious that in the area downstream the structure the horizontal component of velocity (u) takes negative values. The area of these negative values coincides with the recirculation field in each case as shown in Fig. 3. In the rest calculating field the values of the component (u) are always positive, with peak values appearing at the middle of the flow field height (y = 4).

The distribution of the vertical component of velocity for the cases ($LGB^1_{9.6}$) ($LGB^1_{14.0}$) ($LGB^2_{9.6}$) ($LGB^2_{14.0}$) is illustrated in Fig. 5. In the area downstream the structure the vertical component of

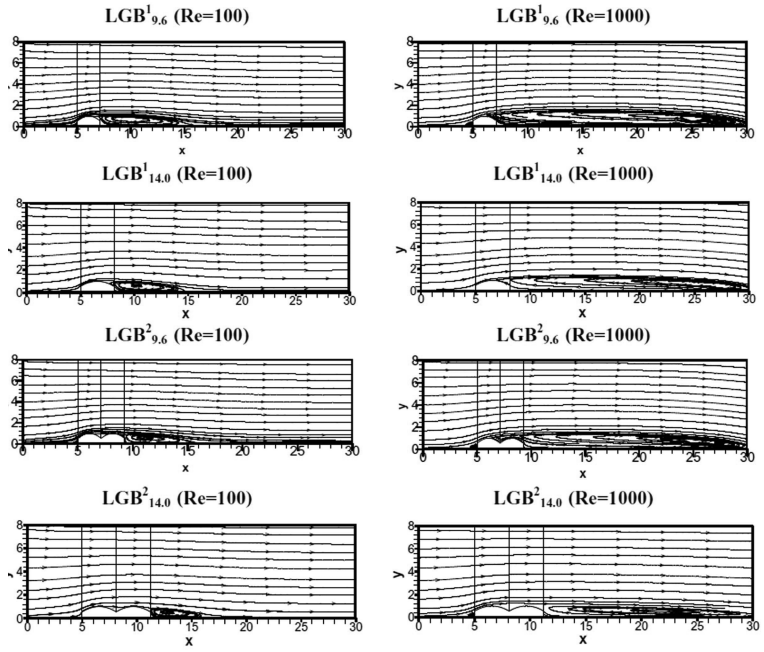

Fig. 3 Streamlines of the flow

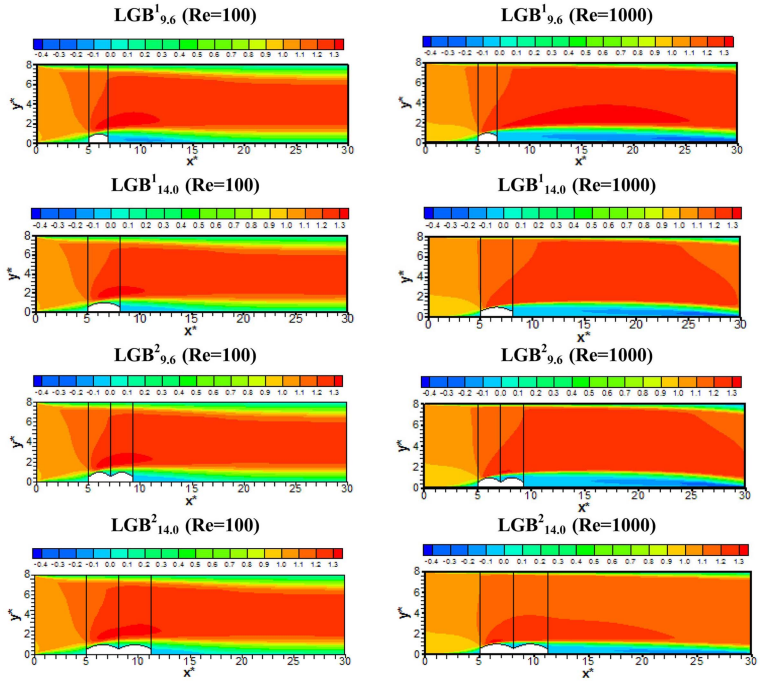

Fig. 4 Distributions of stream-wise velocities (u).

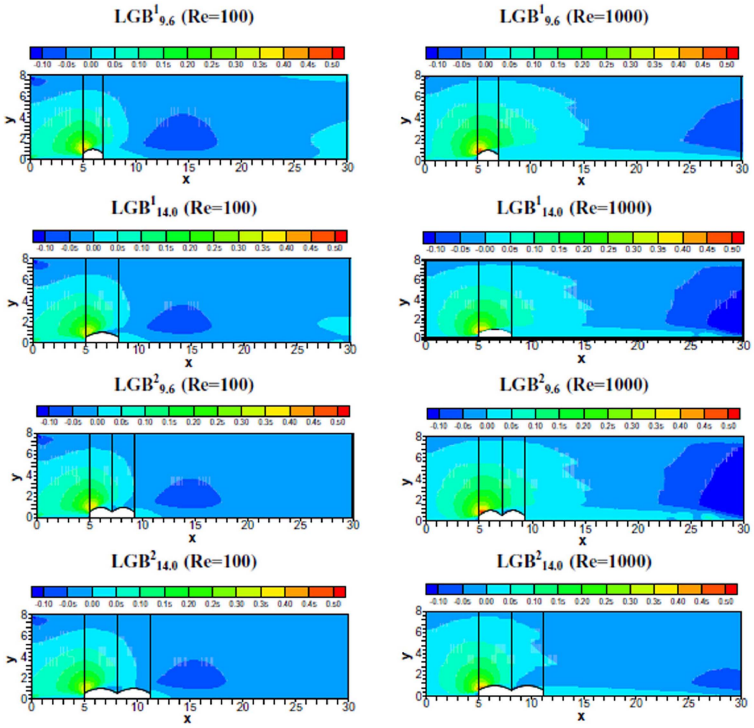

Fig. 5 Distributions of vertical component of the velocity (v)

velocity (v) takes negative values. The negative values of the vertical velocity component appear near the structure for lower *Re* numbers while they tend to move further from the structure for higher Re numbers The maximum values of the vertical velocity component (v) appear at the gutter area at the front of the livestock building and the values are even higher in cases where *Re* number is 1000 as shown in Fig. 5.

3.2 External pressure coefficient (c_{pe})

In Figs. 6 and 7 the aerodynamic pressure coefficients along the external surface of the livestock greenhouse structures are presented. The values of c_{pe} in each point of the roof and for *Re* numbers up to 1500 are presented. In Figs. 6 and 7 it is observed that the distribution of the pressure coefficient for $Re = 1370$ is identical with the one obtained for $Re = 1500$. It has to be noted that execution of computations for $Re > 1500$ did not affect significantly the c_{pe} values which remained at the same values (Data not shown).

It has to be noted that for twin-span constructions, the comparison is performed against EN 13031-1:2001 and not against EC1 because EC1 does not provide values for this type of constructions.

In Fig. 6 the numerical results of $LGB^1_{9.6}$ and $LGB^2_{9.6}$ are compared against the c_{pe} values given by the European standards (EC1 and EN 13031-1:2001) for the same structure design and flow conditions. It is observed that the curves of the pressure coefficient (c_{pe}) for every *Re* number take positive values at the first part of the roof (for $0^o \le \theta \le 20^o$ approximately) and negative values throughout the rest (Fig. 6). This observation is in accordance with the suggested values from European standards for all the situations under study. Specifically, it is confirmed that the curves of

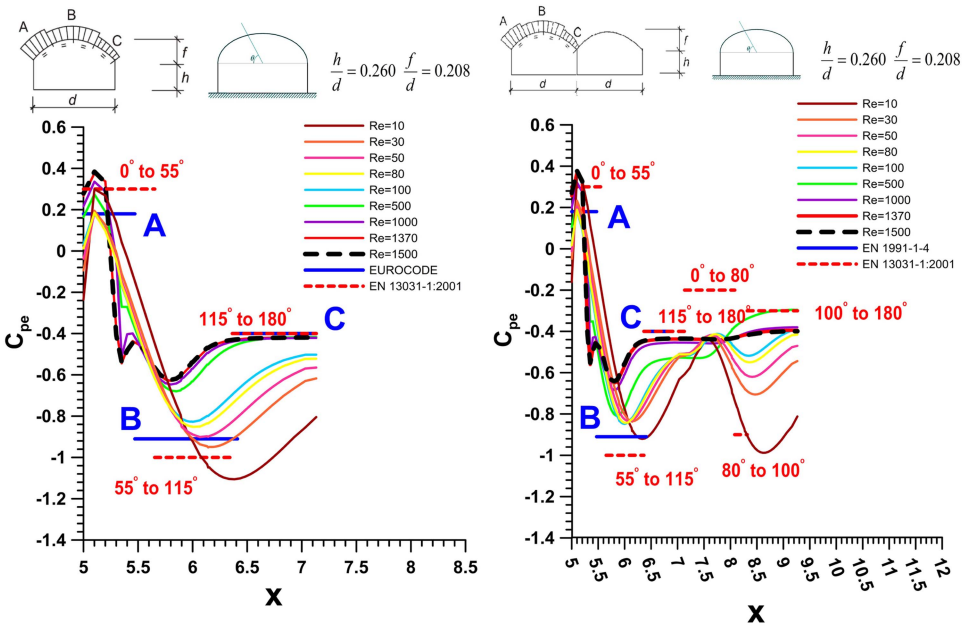

Fig. 6 Distribution of the pressure coefficient c_{pe} on the roof of a livestock greenhouse-type building in the cases $LGB^1_{9.6}$ and $LGB^2_{9.6}$ and for indicative *Re* numbers from 10 to 1500

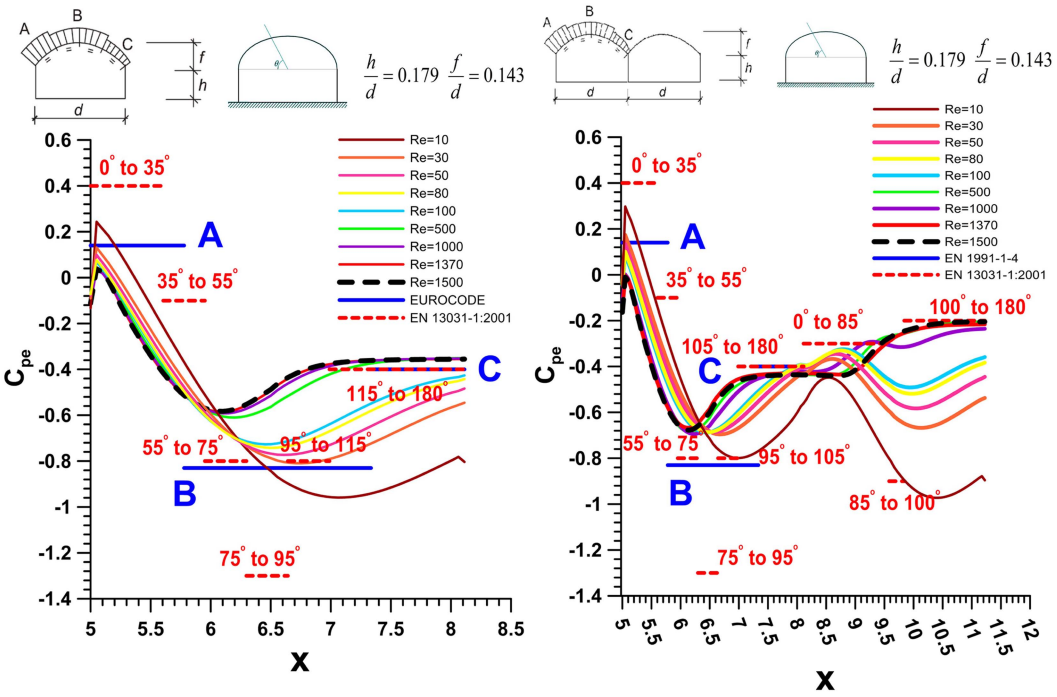

Fig. 7 Distribution of the pressure coefficient c_{pe} on the roof of a livestock greenhouse-type building in the cases $LGB^1_{14.0}$ and $LGB^2_{14.0}$ and for indicative *Re* numbers from 10 to 1500

the pressure coefficient that result from the mathematical model approximate the constant values of region *A* of EC1 and the values of EN 13031-1:2001 for an angle of $0^o \le \theta \le 55^o$, while in region *B*, for an angle of $55^o \le \theta \le 115^o$ the values that the model provides are significantly lesser in absolute value compared to the values that the European standard EC1 provides for high *Re* numbers, while for lower *Re* numbers the values of the model approximate those provided by European standards. In region *C* and for an angle of $115 \le \theta \le 180^o$ the values from the Eurocodes and the calculated ones, coincide for $Re > 500$.

In the case of $LGB^2_{9.6}$, and for higher Re numbers, the absolute values of the output of the model for the second span are higher in the region $0 \le \theta \le 80^o$ while in the region $80^o \le \theta \le 100^o$ they are significantly lesser than those provided by EN 13031-1:2001. The values of EN 13031-1:2001 are approximated better for low *Re* numbers ($Re = 10$). While, for the region $100^o \le \theta \le 180^o$ one can observe better approximation of the Eurocode values for higher Re numbers.

Similar findings and useful conclusions can be derived, also, from the curves of pressure coefficient, shown in Fig. 7, for roofs of greenhouse-type livestock structures for the cases of $LGB^1_{14.0}$ and $LGB^2_{14.0}$.

In Fig. 7, in a similar fashion to Fig. 6, the curves of the pressure coefficients for each *Re* number, assume positive values at the first part of the roof ($0^o \le \theta \le 20^o$ approximately) and negative values in the remaining part of the roof. However, the values of the pressure coefficient decrease in a smoother manner in comparison with $LGB^1_{9.6}$, This decrease continues until the peak of the first span, while after the peak we have an increase in the values of the pressure coefficient.

From Fig. 7 it can be easily seen that the values of the pressure coefficient that result from the

mathematical model approximate the value of region *A* of EC1 but differences are observed in the regions $0^o \le \theta \le 35^o$ and $35^o \le \theta \le 55^o$ of EN 13031-1:2001. In region B, the values of the model are lesser in terms of absolute value compared to the values of the Eurocodes, the largest deviation manifests itself in the region $75^o \le \theta \le 95^o$ in comparison with the values provided by EN 13031-1:2001. In region *C* and for angle values $115^o \le \theta \le 180^o$ satisfactory coincidence exists between the calculated values and the ones obtained from the European standards.

In the case of $LGB^2_{14.0}$ and for the roof of the second span some agreement is observed for angle $0^o \le \theta \le 85^o$ of EN 13031-1:2001 compared with the results of the model, while for angle $85^o \le \theta \le 100^o$ approximation is observed only for $Re = 10$, in the region $100^o \le \theta \le 180^o$ the values of the model approximate to a certain extend the values of EN 13031-1:2001.

From the above observations one can deduce that the largest deviations of the model from the values that are provided by the Eurocodes manifest themselves in region *B* while the highest convergence takes place in the leeward area. In region *B* the values of the model are lesser in absolute value from the ones that are provided by the Eurocodes. It can be considered that the Eurocodes in this area provide conservative values, a similar conclusion was drawn by Blackmore and Tsokri (2006). Additionally, it has been observed that the point in which the largest absolute value of pressure coefficient (c_{pe}) appears around the top of the roof. For small *Re* numbers the maximum absolute value of the pressure coefficient increases and becomes displaced towards the rear part of the roof. This observation has also been confirmed experimentally by Robertson *et al.* (2002) in a wind tunnel with a structure of similar geometry with these in the present study. Furthermore, from a comparison of the curves of Figs. 6 and 7 it can be deduced that as the width of the structure is getting larger the maximum absolute value of the pressure coefficient reduces correspondingly for all Reynolds numbers.

Fig. 8 shows a proposed segmentation of the roof of each unit in all four cases studied in the present work and provides indicative values for the pressure coefficient for each segment. The segmentation was based on the variation of the pressure coefficient's curve for the maximum Reynolds number ($Re = 1500$) for each case. This specific value for the Reynolds number was selected because as it has already been mentioned, the values of the pressure coefficient show only slight variations for larger Re numbers. The suggested value for the pressure coefficient is the mean value of the curve of the pressure coefficient (c_{pe}) for $Re = 1500$ that belong to the respective part of the roof. It is suggested that the proposed segmentation will be a significant aid for the designer-

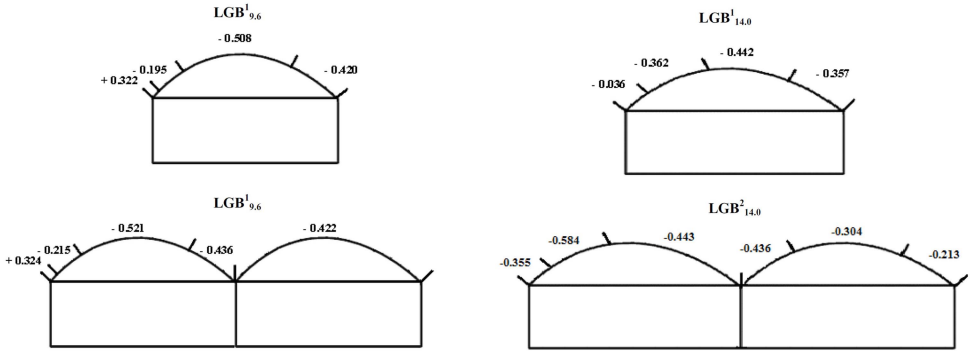

Fig. 8 Suggested segmentation of the roof and indicative pressure coefficients (c_{pe}) corresponding to cases $LGB^1_{9.6}$, $LGB^2_{9.6}$, $LGB^1_{14.0}$ και $LGB^2_{14.0}$

constructor towards the most economical design of a livestock building construction since the pressure coefficient will be already available with relative accuracy for every section of the roof.

It has to be mentioned that there is a need to investigate further the distribution of the air pressure coefficient with the use of mathematical models of unstable flow in three dimensions, so that the approximation of the air pressure coefficients can become more accurate. However, such a numerical procedure requires large amounts of computational effort and computational time.

4. Conclusions

In the present work, the distributions of the air pressure coefficient on the roofs of livestock buildings were calculated. The calculation was aided by the use of a mathematical model that simulates the air flow inside an air-tunnel. The values that came out from the simulation were compared with values provided by European standards (EC1, EN 13031-1:2001). The main outcomes of this study are:

• The calculated values from the model follow in general the variations of the values of the pressure distribution that are provided by the Eurocodes.

• The calculated values for c_{pe} in the leeward area for all cases approximated well the values that are provided by the European standards.

• The c_{pe} values at the top of the roof that are provided by the European standards were higher in terms of absolute value compared to those calculated by the used model in the case of high *Re* numbers. However, for small *Re* numbers the approximation accuracy was satisfactory. Probably, there is a need to review the values of the Eurocodes for this case, since for small *Re* numbers, the air velocity is low and it does not stress the construction.

Based on the results, a segmentation of the roof was suggested for the cases studied and indicatory values of the pressure coefficient were presented for every section, in order to help agricultural engineers to better design livestock buildings.

References

Antoniou, J. and Bergeles, G. (1988), "Development of the reattached flow behind surface-mounted two-dimensional prisms", *J. Fluid. Eng. - T. ASME*, **110**(2), 127-133.

Armaly, B.F., Durst, F., Pereira, J.C.F. and Schonung, B. (1983), "Experimental and theoretical investigation of backward-facing step flow", *J. Fluid Mech*., **127**, 473-496.

Blackmore, P.A. and Tsokri, E. (2006), "Wind loads on curved roofs", *J. Wind Eng. Ind. Aerod*., **94**(11), 833-844.

Boum, G.B.N., Martemianov, S. and Alemany, A. (1999), "Computational study of laminar flow and mass transfer around a surface-mounted obstacle", *Int. J. Heat Mass Tran*., **42**(15), 2849-2861.

CEN. (2001), Comite Europeen de Normalisation, EN 13031-1-2001, *Greenhouses: Design and construction Part 1: Commercial production greenhouses*, Brussels.

CEN. (2005), European Committee for Standardization , *Eurocode 1: Actions on Structures, Part 1-4: General actions - Wind actions*, Brussels.

Dados, J.N., Fragos, V.P., Ntinas, G.K., Papoutsi-Psychoudaki, S. and Nikita-Martzopoulou, C. (2011), "Numerical simulation of airflow over two successive tunnel greenhouses", *Int. Agrophysics*, **25**(4), 333-342.

European Commission website on the Eurocodes, URL link (accessed: 7 December 2011): http://eurocodes.jrc.ec.europa.eu/showpage.php?id=31.

Fragos, V.P., Psychoudaki, S.P. and Malamataris, N.A. (1997), "Computer-aided analysis of flow past a surface-mounted obstacle", *Int. J. Numer. Meth. Fl*., **25**(5), 495-512.
Ginger, J.D. and Holmes, J.D. (2003), "Effect of building length on wind loads on low-rise buildings with a steep roof pitch", *J. Wind Eng. Ind. Aerod*., **91**(11), 1377-1400.
Guirguis, N.M., Abd El-Aziz, A.A. and Nassief, M.M. (2007), "Study of wind effects on different buildings of pitched roofs", *Desalination*, **209**(1-3), 190-198.
Hong, Y.J., Hsieh, S.S. and Shih, H.J. (1991), "Numerical computation of laminar separation and reattachment of flow over surface mounted ribs", *J. Fluid. Eng. - T. ASME*, **113**(2), 190-198.
John, V. and Liakos, A. (2006), "Time-dependent flow across a step: the slip with friction boundary condition", *Int. J. Numer. Meth. Fl*., **50**(6), 713-731.
Kotsopoulos, T.A. and Martzopoulou, A.G. (2007), "Modern tendency of livestock buildings design in Greece and their effect on the environment", (Eds. Kungolos, A., Aravossis, K., Karagiannidis, A. and Samaras, P.), *Proceedings of the SECOTOX Conference and the International Conference on Environmental Management Engineering, Planning and Economics*, GRAFIMA, Skiathos, Greece, 2533-2538.
Kozmar, H. (2011), "Wind-tunnel simulations of the suburban ABL and comparison with international standards", *Wind Struct*., **14**(1), 15-34.
LME, London Metal Exchange, URL link (accessed: 7 December 2011): http://www.lme.com/ steel/steel_ price_graphs.asp.
Lopes, M.F.P., Paixão Conde, J.M., Glória Gomes, M. and Ferreira, J.G. (2010), "Numerical calculation of the wind action on buildings using Eurocode 1 atmospheric boundary layer velocity profiles", *Wind Struc*t., **13**(6), 487-498.
Malamataris, N.A. (1991), *Computed-aided analysis of flows on moving and unbounded domains: phase-change fronts and liquid leveling*, University of Michigan.
Mistriotis, A. and Briassoulis, D. (2002), "Numerical estimation of the internal and external aerodynamic coefficients of a tunnel greenhouse structure with openings",*Comput. Electron. Agr*., **34**(1-3), 191-205.
Nikita – Martzopoulou, C. (2007), "*New trends in animal housing in Greece: greenhouse type livestock buildings, animal housing in hot climate*", CIGR, Cairo, Egypt, 115-116.
Norton, T., Grant, J., Fallon, R. and Sun, D.W. (2009), "Assessing the ventilation effectiveness of naturally ventilated livestock buildings under wind dominated conditions using computational fluid dynamics", *Biosyst. Eng*., **103**(1), 78-99.
Papanastasiou, T.C., Malamataris, N. and Ellwood, K. (1992), "A new outflow boundary- condition", *Int. J. Numer. Meth. Fl*., **14**(5), 587-608.
Psychoudaki, S.P., Laskos, V.N. and Fragos, V.P. (2005), "Numerical analysis of a Viscous Flow over a mounted Parabolic Body", *IASME Transactions*, **2**, 1207-1216.
Reichrath, S. and Davies, T.W. (2002), "Computational fluid dynamics simulations and validation of the pressure distribution on the roof of a commercial multi-span Venlo-type glasshouse", J. *Wind Eng. Ind. Aerod*., **90**(3), 139-149.
Robertson, A.P., Roux, P., Gratraud, J., Scarascia, G., Castellano, S., de Virel, M.D. and Palier, P. (2002), "Wind pressures on permeably and impermeably-clad structures", J. *Wind Eng. Ind. Aerod*., **90**(4-5), 461-474.
Shklyar, A. and Arbel, A. (2004), "Numerical model of the three-dimensional isothermal flow patterns and mass fluxes in a pitched-roof greenhouse", *J. Wind Eng. Ind. Aerod*., **92**(12), 1039-1059.
Tieleman, H.W. (2003), "Wind tunnel simulation of wind loading on low-rise structures: a review", *J. Wind Eng. Ind. Aerod*., **91**(12-15), 1627-1649.
Wright, N.G. and Easom, G.J. (2003), "Non-linear k-epsilon turbulence model results for flow over a building at full-scale", *Appl. Math. Model*, **27**(12), 1013-1033.
Zienkiewicz, O.C., Taylor, R.L. and Nithiarasu, P. (2006), *Finite element method for fluid dynamics*, 6th, Elsevier.

CC

Nomenclature

Symbols	
c_{pe}	external pressure coefficient
d	length, span
f	length between gutter and ridge
h	length of column (between foundation and gutter)
I	identity matrix
p	Pressure
p_o	reference pressure
P_o	pressure intensity (Nm^{-2})
L	length of the ridge above ground level (m)
R_c^i, R_M^i	weighted residuals
Re	Reynolds number
S	surface of the element
T	stress tensor of the Newtonian fluid
u	velocity vector of the fluid
u	stream-wise velocity
v	cross-wise velocity
V	volume of the element
V	uniform approaching velocity of the fluid (ms^{-1})
x, y	Cartesian coordinates

Greek letters	
v	kinematic viscosity of the fluid (m^2s^{-1})
ρ	density of the fluid (Ns^2m^{-4})
Ψ^i, Φ^i	linear and quadratic basic functions